

# Study on Ultimate Limit of Steel Roof Truss at Nuclear Power Plant

**T. Suzuki, H. Kaneko & M. Kanchi**  
*Takenaka Corporation, Japan*

**Y. Nukui, A. Imamura & T. Terayama**  
*Tokyo Electric Power Company, Japan*



## SUMMARY

In the seismic safety evaluation of the nuclear power plants, the reasonable specification of the ultimate performance is important and required. However, the ultimate performance of steel roof trusses at nuclear power plants is not clear. The reason is because the steel roof trusses at nuclear power plant are designed to remain nearly elastic range against seismic motions for design. So, the purpose of this study is to clarify the ultimate performance of large span roof truss at nuclear power plant, for advanced safety evaluations.

First, in this study, the static loading test of large-scale specimens, that imitate real roof truss, is done. Then, behavior and deformation capacity of roof truss in large deformation area are examined. And by analytical method, the correspondence of the damage of truss member and whole behavior is confirmed.

*Keywords: Roof truss, Ultimate limit, Static loading test, Deformation capacity, Nuclear power plant*

## 1. INTRODUCTION

In Japan, steel trusses including roof trusses at nuclear power plant had been generally designed by considering dynamic horizontal seismic motion and static vertical seismic force, until the “Evaluation Guidelines for Seismic Design Relating to Nuclear Power Reactor Facilities” was revised. Then, Trusses were designed such that buckling and yielding do not occur in their individual members such as upper and lower chord members and web members (i.e., diagonal and lattice members) under these seismic forces. However, according to a revision to the “Evaluation Guidelines for Seismic Design Relating to Nuclear Power Reactor Facilities”, the horizontal seismic motion used for evaluating earthquake-proof safety may be large. Moreover, dynamic vertical seismic motion should be considered. Then, the large-span roof trusses in existing reactor buildings will probably enter the plastic region against these seismic motions. To further improve reliability of evaluating the earthquake-proof safety of nuclear power plants, a rational and clear indication of the ultimate limit performance and seismic safety margin is required. To this end, at large-span roof trusses in existing reactor buildings, it is important to clarify their behavior in large deformation areas and their ultimate limit.

The purpose of this study is to determine the ultimate limit of large-span roof trusses in existing reactor buildings against seismic inputs for an advanced evaluation of earthquake-proof safety. First, a scaled-down test piece that corresponds to an actual roof truss is fabricated. Next, a static load test that simulates vertical dynamic loads, which greatly influence the collapse behavior of a truss, is conducted. Using this test, the behavior and deformation performance of the roof truss in large deformation areas are clarified. Then, an analysis model that can simulate the experimental results with high accuracy is constructed, and an analytical study of the correspondence between damage to a single truss member and overall behavior is conducted.

## 2. STATIC LOAD TEST FOR A STEEL ROOF TRUSS SUBJECTED TO VERTICAL LOAD

### 2.1. Test plan

As shown in Figure 1, roof trusses in existing nuclear power plants in Japan are categorized as Pratt and Warren trusses. Therefore, we decided to experimentally verify the ultimate behavior of both trusses. The test pieces, one of the Pratt truss and the other of the Warren truss, represented one structural plane of the actual roof truss. To accurately simulate the actual behavior, the test pieces were fabricated on a scale as large as the test facilities would allow, which was 38% of actual size. Moreover, the assumed seismic load was replaced with a static load and an incremental cyclic load was applied.

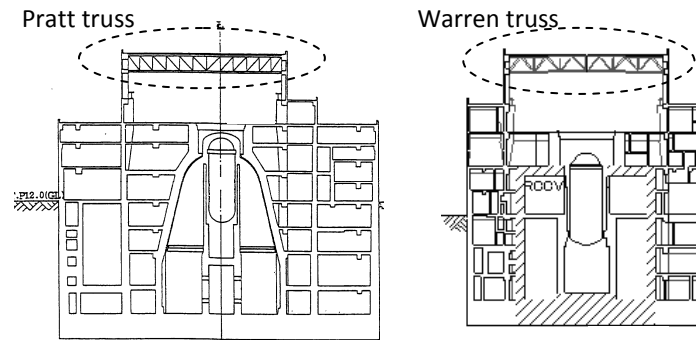


**Figure 1.** Types of roof trusses in nuclear power plant buildings (reactor buildings)

When the input is increased further, many members are at a risk of damage due to vertical seismic motion. Therefore, we decided to focus on vertical load in this experiment. Figure 2 shows a model of dynamic load distribution for vertical seismic motion. The actual distribution has a parabolic shape; however, triangular distribution is applied where the center of the truss span is at a maximum. By assuming a triangularly distributed static load, we consider dynamic effects.

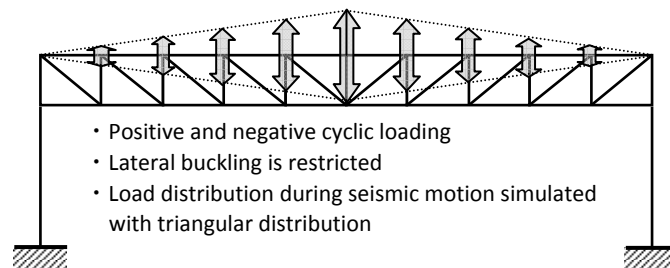


**Figure 2.** Triangular distribution model of dynamic vertical load distribution

The configuration of each test piece is shown in Figure 3. Because of the symmetrical conditions, the test piece constituted only half of the truss from the center point ① of the truss. Steel sheets with a thickness of more than 4.5 mm were used for the test pieces. In order to meet the flexural buckling strength, the radius of gyration for each member was set to correspond to the object model. When the width–thickness ratio did not correspond to the object model, it was set smaller. The cross sections of the steel columns were made to correspond to the elastic bending rigidity of the columns in the object model.

The mechanical characteristics of the steel are the same as those of the actual truss (Table 1). The number of high-strength bolts is set such that the slip-proof strength is greater than the yield strength of the base material. Moreover, the section with a lack of cross section owing to bolt holes is either widened or a steel sheet is spliced so that the effective sectional area of the base material becomes

equal. A detailed drawing of the example of a typical joints at which the diagonal member between ② and ③ passes through ② is shown in Figure 4. In both Pratt and Warren trusses, the diagonal member between ② and ③ was the first member to produce buckling. Moreover, in the Warren truss, a tear-off fracture occurs at this particular joint.

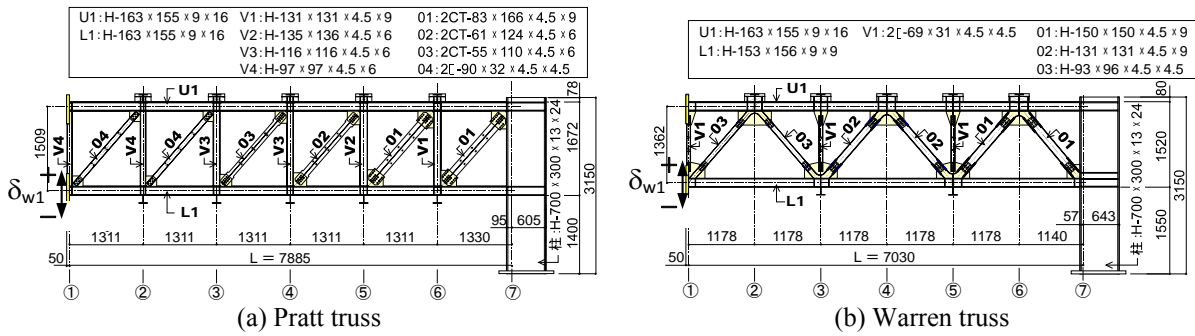


Figure 3. Geometries of the test piece

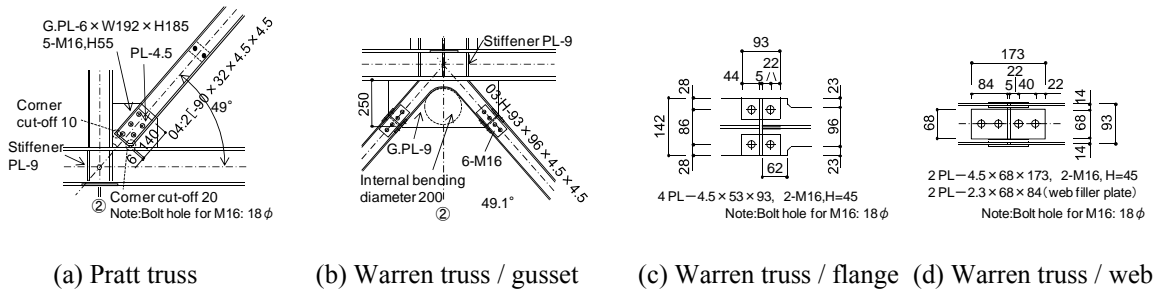


Figure 4. Detailed drawings of the joints of the test piece (diagonal member between ② and ③)

Table 1. Mechanical characteristics of the materials

Sheet thickness (mm)	Steel type	Yield strength (N/mm <sup>2</sup> )	Tensile strength (N/mm <sup>2</sup> )	Applied member
4.5	SS400	333	466	Pratt truss O4 only
4.5	SM490	399	531	Pratt truss other than O4
6	SM490	415	557	Diagonal members/lattice members
9	SM490	424	547	Diagonal members/lattice
12※	SM490	413	551	Reinforced sheet/force application device
16	SM490	378	547	chord member

※ mill sheet value

The loading device is shown in Figure 5. To apply symmetrical force, a linear slider that can slide vertically is set on the test wall. Lateral restricting jigs are installed at the node position, where lateral buckling is restricted by the sub-truss or other members. Furthermore, weights are set to reproduce the roof's weight. The size of the weights is calculated from the snow load during an earthquake as well as stationary load of the roof framework.

A triangular distribution load corresponding to vertical seismic motion is applied to the nodes of the upper chord member by five hydraulic jacks (② to ⑥) suspended from the rigid frame. The load ratios for the jacks are maintained as shown in Table 2. Because of the constraints of the test facilities, the load that generally should be acted on ① is acted on ②. The hydraulic jack load is adjusted to satisfy the load ratio at each loading step.

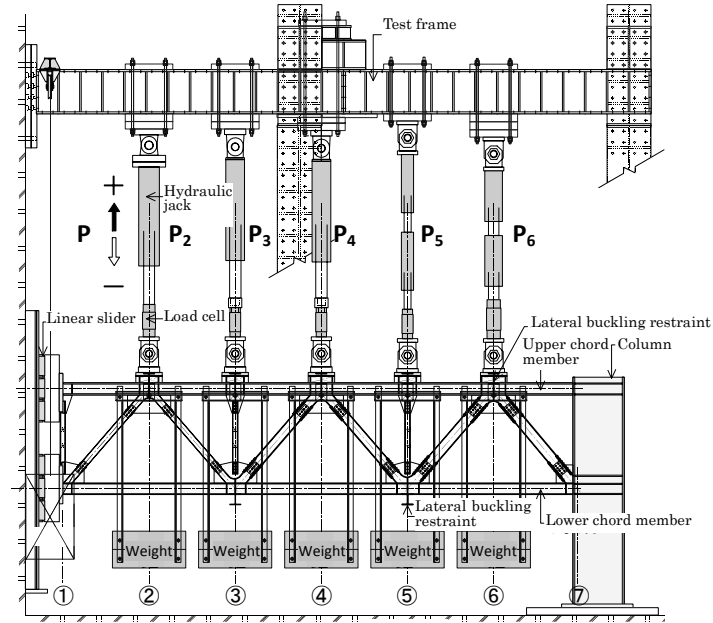


**Figure 5.** Test piece and Loading device

**Table 2.** Node load ratios

Jack		P2	P3	P4	P5	P6	Total
Ratio	Pratt	0.44	0.22	0.17	0.11	0.06	1.00
	Warren	0.45	0.22	0.17	0.11	0.05	1.00

Force was applied according to the following procedure. First, before incremental cyclic loading, weights (nodal load 40 kN) equivalent to the roof truss stationary load were loaded onto the test piece. The weights were suspended from each node position through lateral support jigs. A slider weight of 20 kN acted on the center of the span. After the weights were loaded, truss deformation was set to 0. In this state, positive and negative incremental cyclic loading, maintaining triangular distribution load, was conducted. Figure 6 shows the loading pattern. The downward load is indicated as the negative load, and the application of force began from the negative side. The displacement measured by a displacement meter installed on the lower chord member at ① at the center of the span is  $\delta_{w1}$  (the downward direction is negative), and the value divided by the length of the test piece  $L$  (shown in Figure 3) is the deflection angle  $R_{w1}$ .

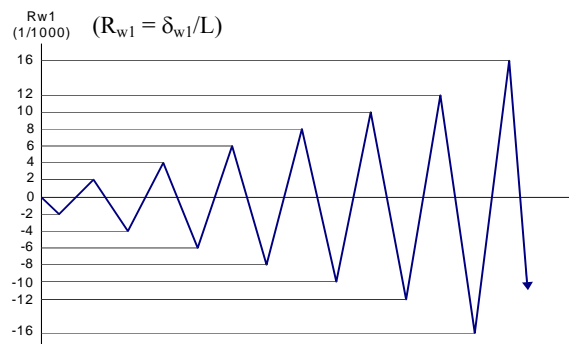


**Figure 6.** Loading pattern

## 2.2. Experimental results

The deflection angle when the weights were loaded was  $-2.1/1000$  for the Pratt test piece and  $1.5/1000$  for the Warren test piece.

The load–deformation relationship for the Pratt test piece is shown in Figure 7(a). The vertical axis shows the total load in a vertical direction from the jacks, and the horizontal axis shows the deflection angle  $R_{w1}$ . During positive loading, flexural buckling occurs simultaneously in the three diagonal members between ② and ⑤ (Figure 7(b)). And the buckling occurs toward the deflection angle target peak value of  $R_{w1}=8/1000$ . Hence, strength is temporarily reduced. However, by converting to a mechanism with Vierendeel-type truss beams constructed from chord members and lattice members, stable behavior is displayed. In other words, the upper and lower chord members and the lattice members act as flexural members and bear the shear force that the diagonal members can no longer bear (hereafter, this effect is referred to as the Vierendeel effect). During negative loading, the diagonal members are restored to a linear state by tensile force. So, a truss mechanism is formed, and stable behavior is displayed. However, strength is reduced from local buckling of lattice members ③ to ⑤ (Figure 7(c)) and approximately two-thirds of the negative-loading-side maximum strength is retained.

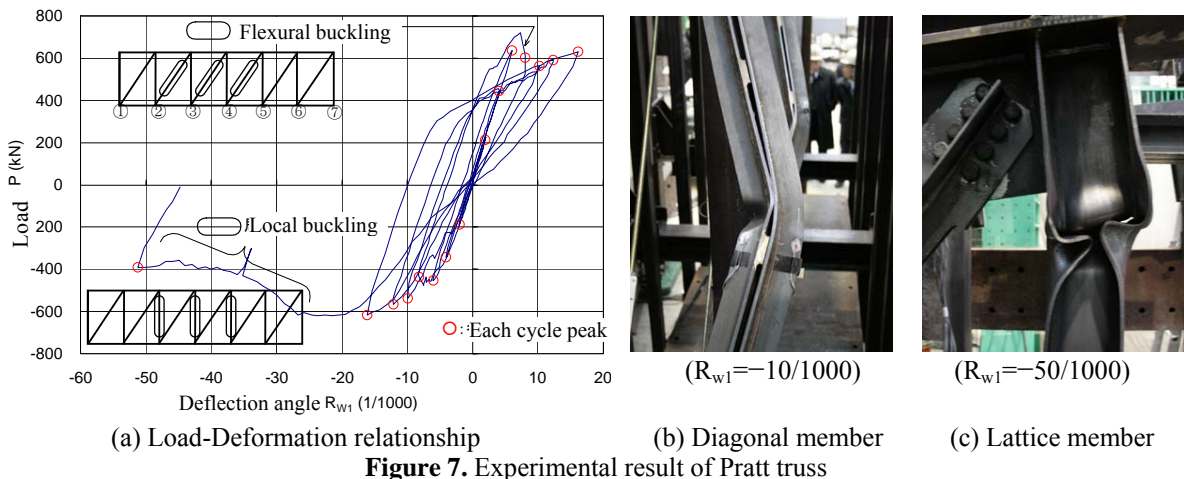


Figure 7. Experimental result of Pratt truss

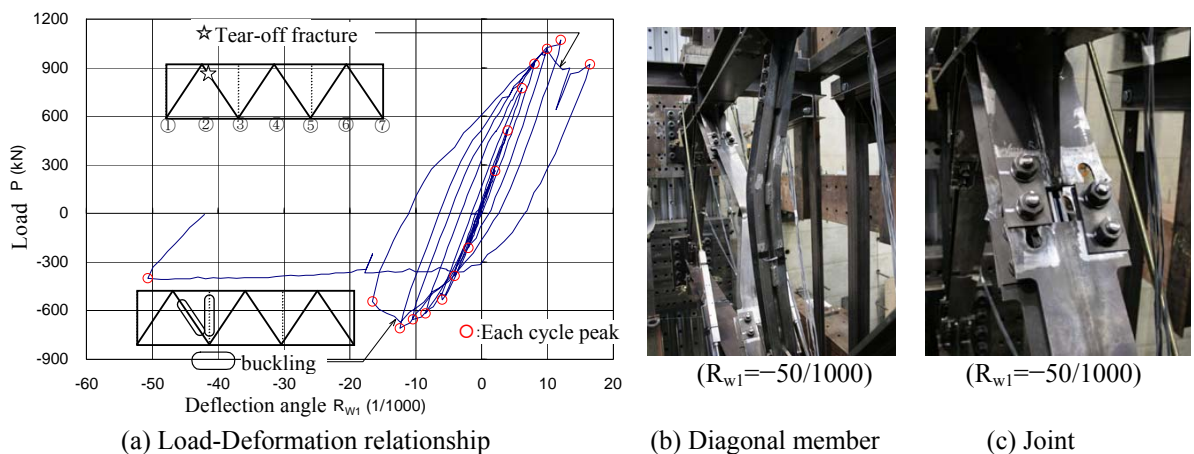


Figure 8. Experimental result of Warren truss

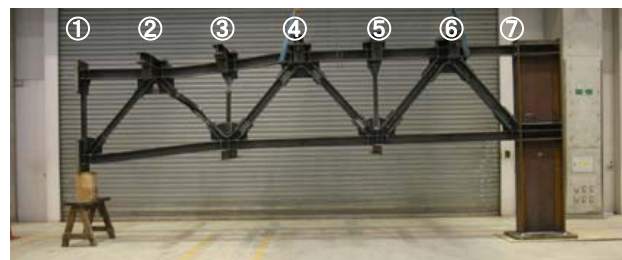
The load-deformation relationship for the Warren test piece is shown in Figure 8(a). At  $R_{w1} = -12/1000$  of the cycle toward the  $R_{w1} = -16/1000$  during negative loading, flexural buckling occurs in the diagonal member between ② and ③, and lattice member located at ③ (Figure 8(b)). Then

strength is reduced. However, unstable behavior is not observed afterwards. At  $R_{w1} = 10/1000$  during the deformation cycle to the positive loading peak of  $R_{w1} = 16/1000$ , a tear-off fracture occurs in the diagonal member base materials on the upper chord member side and the gusset plate side (Figure 8(c)), and strength is reduced. After that, during negative loading, deformation is applied up to  $R_{w1} = -51/1000$  and approximately half of the negative-loading-side maximum strength is retained.

Figure 9 shows an overview of the test piece after the experiment was complete. The experiment ended on negative loading; therefore, the three diagonal members between ② and ⑤ of the Pratt test piece, which exhibited flexural buckling, are restored to a linear state. However, the lattice members from ③ to ⑤, exhibit local buckling and large deformation is produced. In the Warren test piece, only the diagonal members between ② and ③ and the lattice member at ③ are deformed locally by flexural buckling.



(a) Pratt test piece



(b) Warren test piece

**Figure 9.** Overview of test pieces after experiment completion

In this experiment, a triangularly distributed load was subjected to scaled-down test pieces of steel roof trusses, and elastic–plastic behavior was verified. The effective slenderness ratio of the diagonal members of the test pieces used in this experiment was 26–128 for the Pratt test piece and 31–54 for the Warren test piece. The width–thickness ratio was ranked from FA to FB, and both test pieces exhibited an almost stable hysteresis loop up to  $R_{w1} = \pm 10/1000$ . Furthermore, even when the deformation reached the deflection angle of  $R_{w1} = -50/1000$ , both test pieces maintained the stationary load and did not collapse. It was verified that they could bear vertical seismic force of more than half their maximum strength, maintaining stationary load.

### 3. EFFECT OF DAMAGE TO SINGLE TRUSS MEMBERS ON COLLAPSE BEHAVIOR

Based on the experimental results obtained in the previous section, buckling of a single member is not directly linked to the collapse of a roof truss. For the evaluation of the ultimate limit of a roof truss, buckling of a single member is permissible. However, in order to set the permissible value, it is important to study the relationship between the single member buckling behavior and the overall behavior of roof truss in more detail. Therefore, the purpose of this section is to understand analytically the relationship between the single member buckling behavior and the overall behavior of roof truss. To this end, we first create an analysis model that simulates the experimental results with high accuracy.

### 3.1. Simulation analysis of the experimental results

Here we provide an overview of the analysis. For diagonal members and lattice members, the truss element is applied. For these buckling behaviours, the modified Wakabayashi model (Taniguchi et al (1991)) is used. And flexural rigidity is not taken into account. The modified Wakabayashi model is a model in which the initial buckling strength and the strength degradation curve after buckling for the Wakabayashi model (Shibata, Wakabayashi (1984)) are modified. Furthermore, the effective buckling length for defining initial buckling strength is calculated by considering end constraints such as the gusset plate. The calculated effective buckling length was 0.85 times the length of the diagonal member between ② and ③ of the Pratt truss and 0.67 times the length of the diagonal member between ② and ③ of the Warren truss. These effective buckling coefficients for analysis are applied to all the diagonal members. The correspondence between the calculated buckling length and the actual member is shown in Figure 10. In the case of the Pratt truss, the calculated buckling length corresponds to the actual length of the diagonal member without the gusset portion, and to the buckling length determined from the collapse mode. And, in the case of the Warren truss, the calculated buckling length corresponds to between both edges of the splice plate. These lengths also correspond to the buckling length determined from the collapse mode. Furthermore, the zones outside the buckling length range are treated as rigid zones during analysis, and are modelled as rigid elements.

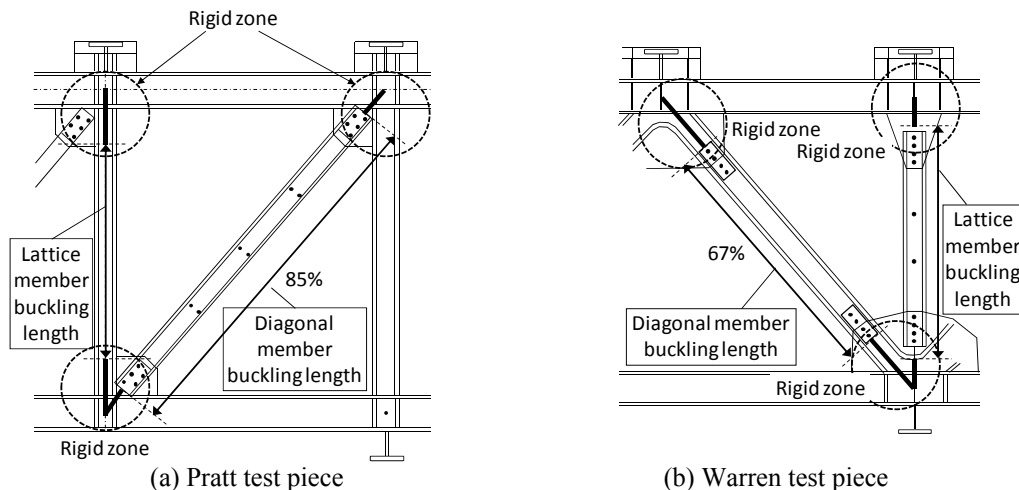


**Figure 10.** Member buckling lengths and rigid zone setting

The buckling length of the lattice member is determined as follows, with reference to the joint of the test piece and the collapse shape during the experiment. The Pratt truss lattice member buckling length is determined from the joint state of the test piece. As such, it is the length except the zones where the gusset plates are settled. The Warren truss lattice member buckling length is the distance between the sections regarded as rigid zones where the longitudinal ribs are mounted on the gussets (refer to Figure 10). It corresponds to the collapse shape (refer to Figure 9(b)).

In the case of the upper and lower chord members, a beam element with rigid-plastic hinge end is used. And rigid-plastic hinge is set such that flexural yielding occurs under the fully plastic moment obtained from the member cross section. Furthermore, strain hardening is not considered. Based on the material test results, the degree of yield stress for the material was set at  $413 \text{ N/mm}^2$  (average value from  $t = 4, 5, 6, \text{ and } 9 \text{ mm}$ ) for SM490 and at  $333 \text{ N/mm}^2$  for SS400. Moreover, the 40 kN weights mounted on each loading point as stationary loads and the weight of the slider at the center of the span (20 kN) are considered as concentrated loads.

Comparisons of the experimental results and simulation analysis are shown in Figure 11. In the case of the load displacement relationship for the Pratt truss, although strength deterioration due to buckling

occurs slightly earlier in the analysis, the analysis accurately simulates the experimental results to the ultimate state of the final loop.

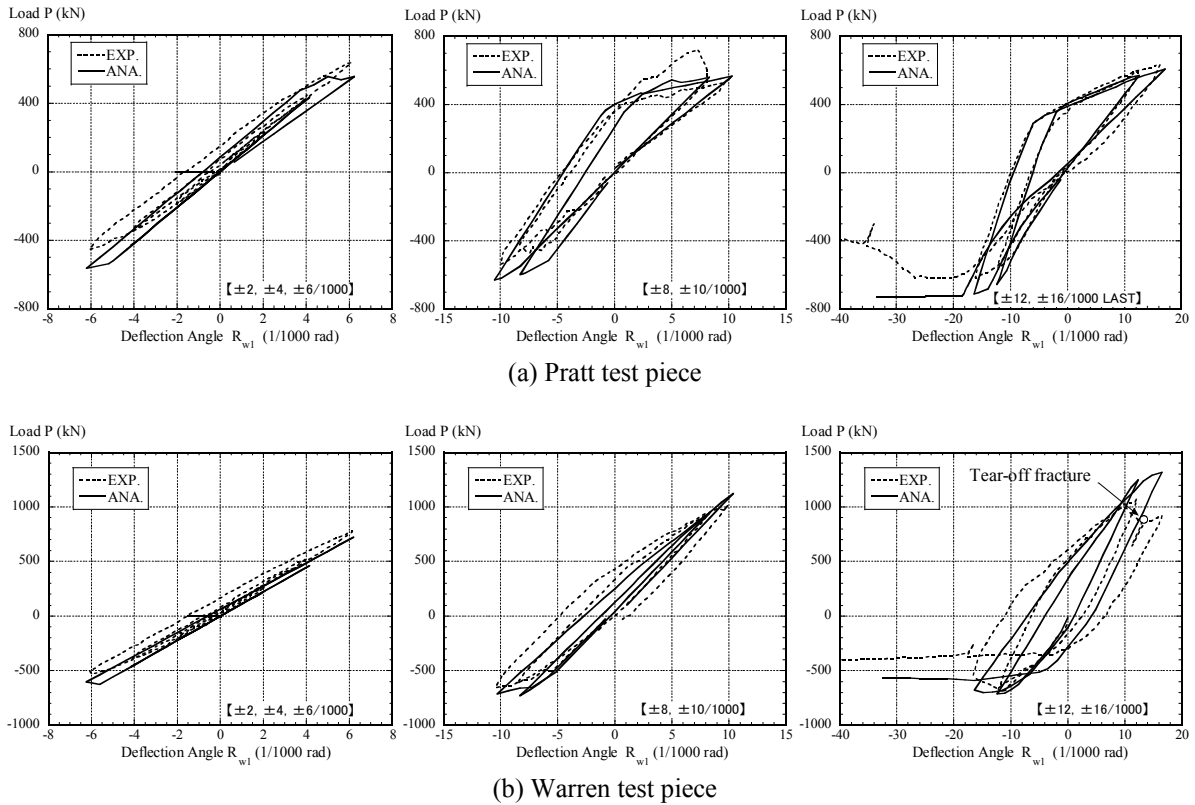


**Figure 11.** Comparisons of the experimental result and simulation analysis

In contrast, in the case of the load displacement relationship for the Warren truss, the loop area for the experimental results becomes slightly large compared with the analytical results from the small amplitude level of  $\pm 6/1000$ . The effect of the bolt slip behavior can be considered as the main causes of this difference. Actually, from the  $\pm 6/1000$  loop, bolt slip noise is verified in both positive and negative directions. Furthermore, accuracy of analysis deteriorates from the  $\pm 16/1000$  loop where a tear-off fracture is generated in the joint. However, the peak point for each cycle is analyzed accurately. It can be said that this analysis model has the required analysis accuracy for taking into consideration the correspondence between the damage state of the single member and the overall behavior. Especially, it can be said that sufficient analysis accuracy is achieved, within the  $\pm 10/1000$  range.

### 3.2. Correspondence between damage to an individual member and overall behavior

Using the analysis results from the simulation analysis model configured in the previous section, we examine the correspondence between the damage state of a single member and the overall behavior. Tables 3 and 4 show the maximum average axial strain (hereafter referred to as equivalent axial strain) and the ductility ratio (maximum equivalent strain/yield strain) at each force application cycle for the diagonal member between ② and ③ (the first member to convert to plastic and the one with the most damage) obtained from analysis. Furthermore, the equivalent axial strain, converted to a non-dimensional value using the initial buckling strain, is also shown for the compression side for reference. At the  $\pm 10/1000$  loop where the truss beam exhibits sufficient load bearing capacity even though rigidity is reduced because of plasticization, the compression side maximum equivalent axial strain is 0.59% (ductility ratio 3.6) for the Pratt truss and 1.47% (ductility ratio 7.3) for the Warren truss.

Moreover, Tables 3 and 4 also show the maximum concentrated strain of the diagonal member between ② and ③. This is calculated from compressive maximum equivalent axial strain with the method proposed by Takeuchi et al (2008). At the  $\pm 16/1000$  loop, the maximum concentrated strain is 9.60% for the Pratt truss and 12.5% for the Warren truss.

**Table 3.** Damage to diagonal member between ② and ③ (Pratt test piece)

Load cycle		Tension side		Compression side		
No.	$R_{w1}$	Equivalent axial strain	Ductility ratio	Equivalent axial strain	Ductility ratio	Concentrated strain
1	2/1000	0.08%	0.5	0.01%	0.1(0.1※)	0.07%
2	4/1000	0.13%	0.8	0.06%	0.4(0.8※)	0.18%
3	6/1000	0.23%	1.4	0.28%	1.7(3.9※)	0.39%
4	8/1000	0.39%	2.4	0.43%	2.6(6.1※)	0.48%
5	10/1000	0.56%	3.4	0.59%	3.6(8.3※)	0.56%
6	12/1000	0.70%	4.3	0.80%	4.9(11.2※)	0.57%
7	16/1000	0.99%	6.1	1.21%	7.4(17.0※)	9.60%

※ Equivalent axial strain/initial buckling strain in brackets

**Table 4.** Damage to diagonal member between ② and ③ (Warren test piece)

Load cycle		Tension side		Compression side		
No.	$R_{w1}$	Equivalent axial strain	Ductility ratio	Equivalent axial strain	Ductility ratio	Concentrated strain
1	2/1000	0.01%	0.1	0.06%	0.3(0.6※)	0.40%
2	4/1000	0.05%	0.2	0.09%	0.4(1.0※)	0.48%
3	6/1000	0.05%	0.2	0.53%	2.6(5.5※)	6.96%
4	8/1000	0.15%	0.7	1.00%	5.0(10.5※)	9.18%
5	10/1000	0.35%	1.7	1.47%	7.3(15.4※)	10.6%
6	12/1000	0.53%	2.6	1.82%	9.0(19.1※)	11.4%
7	16/1000	0.74%	3.7	2.37%	11.8(24.8※)	12.5%

※ Equivalent axial strain/initial buckling strain in brackets

Figure 12 shows the relationship between the axial stress and axial strain for the diagonal truss between ② and ③.

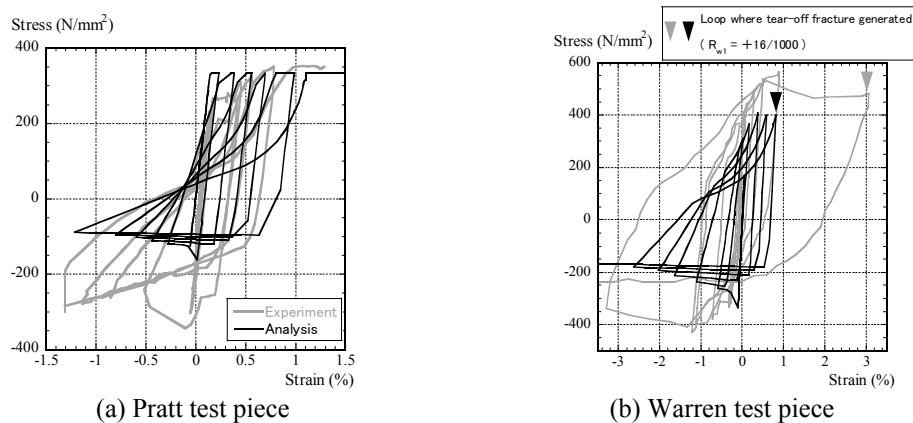


**Figure 12.** The relationship between the axial stress and strain for the diagonal member between ② and ③

The solid black line shows the analysis values and the solid gray line shows the experimental values. In both figures, the tension side is set as positive. The experimental values for strain are obtained from the displacement gauge mounted on the aforementioned diagonal member, and the stress is determined on the assumption that diagonal members bear all the shear force acting between ② and ③, which is calculated from the total load. Therefore, because shear force which the upper and lower chord

members shares is added in the case of experimental values for stress, the analysis values do not correspond to the experimental values. In contrast, the strain values for both the Pratt truss and the Warren truss at the peak of each loop considerably correspond for analysis and experiment. However, the strain values of experiment for the Warren truss become larger than that of analysis from the loop when the tear-off fracture, which is not considered in the analysis, is generated.

When the history of the single member obtained from the analysis is verified, it is found that the strength of the single member deteriorates. In contrast, even when there is buckling and strength deterioration during analysis, the experimental values have positive rigidity and the load is increased. This is because the load values of experiment in the figure include not only the burden share of the diagonal member, but also the burden share for the upper and lower chord members. This diagonal member strength deterioration is supported by the upper and lower chord members because of the Vierendeel truss effect. Therefore the shear force deformation relationship between ② and ③ is stable and as a result the overall displacement relationship history is also stable, as shown in the previous section.

#### 4. CONCLUSION

In this study, for evaluation of the ultimate limit of large-span roof trusses at nuclear power plant, a static load test is conducted. Then, an analytical study of the correspondence between damage to a single truss member and overall behavior is conducted. From the study, the following results were obtained.

(1) A triangular distribution load that simulates dynamic seismic motion was loaded on scaled-down test pieces of a Pratt truss and a Warren truss that represented large-span roof trusses in existing reactor buildings; in addition, the elastic-plastic behavior was verified. Both test pieces exhibited an almost stable hysteresis loop up to a deflection angle of 1/100. Although there was significant buckling deformation in the truss diagonal members, it was verified that both test pieces had the capacity to bear a stationary load up to the large deformation range of a deflection angle of 5/100.

(2) An effective buckling length that considered the bonding type of the joint was set, and a simulation analysis model that could accurately simulate the static loading test results was developed. A study was conducted to establish a correspondence between the damage to each truss member and the overall behavior. It was verified that the buckling of the diagonal and lattice members does not correspond to the ultimate limit of the overall truss structure.

#### ACKNOWLEDGEMENT

This study is a parts of the “Research and Studies on Ultimate Strength of Nuclear Power Plants“ which was carried out under the sponsorship of 12 Japanese electric companies. The authors would like to express their thanks to all the persons involved.

#### REFERENCES

- Taniguchi H., Kato B., et al (1991), Study on Restoring Force Characteristics of X-shaped Braced Steel Frames, *Journal of Structural Engineering*, **37B**, 303-316
- Shibata M., Wakabayashi M. (1984), Mathematical expression of Hysteretic Behavior of Braces : Part 2 Application to Dynamic Response Analysis, *Journal of Structural and Construction Engineering (Transaction of AIJ)*, **No.320**, 29-34
- Nuclear Safety Commission (2006), Evaluation Guidelines for Seismic Design Relating to Nuclear Power Reactor Facilities
- Takeuchi T., et al (2008), Cumulative Cyclic Deformation Capacity of H-section Braces with Local Buckling, *Journal of Structural and Construction Engineering (Transaction of AIJ)*, **No. 632**, 1875- 1882